

Spontaneous radiation from relativistic electrons in a tapered Apple-II undulator

CHEN Mingzhi HE Jianhua*

Shanghai Institute of Applied Physics, Chinese Academy of Sciences, Shanghai 201800, China

Abstract This paper presents most properties of radiation from a tapered Apple-II undulator. The study demonstrates that tapering an Apple-II undulator can broaden the harmonic bandwidth and the performance of polarization is also excellent at the broadened energy range. So Apple-II undulator can be tapered to provide more convenience for energy scan experiment.

Key words Apple-II undulator, Tapered undulator, Variable polarization, Simulation calculation

1 Introduction

Radiation of particular polarization is a must for magnetic circular dichroism (MCD) and other experiments. A number of authors have proposed types of undulators that generate different polarized radiations to meet this particular demand^[1-11]. Apple-II undulator, proposed by S. Sasaki in 1994^[1], is the most popular scheme among them. Properties of the radiation from an Apple-II undulator have been well studied^[1,10,11,14,15].

In some experiments, there is a need to scan over an energy range that is broader than the intrinsic bandwidth of the radiation harmonic. Therefore, the peak harmonic energy must be tuned synchronously in the experiment. One general method is to change the magnetic gap accordingly. However, changing the magnetic gap affects the beam dynamics. Furthermore, experimental paces may be limited by the rate at which the magnetic gap and monochromator are tuned together.

Another method to provide a broader energy range of radiation is to tune the magnetic gap and taper an undulator^[12,13]. However, there have been fewer articles on radiation properties of a tapered Apple-II undulator. Some authors have described properties of radiation from a tapered planar/helical undulator^[12,13,16], but these results cannot be directly applied to

tapered Apple-II undulator, because the ratio of the transverse magnetic field strength B_x and B_y varies along the axis in a tapered Apple-II undulator (see Section 2), while the ratio is constant in a tapered helical undulator. Studies on how the varying ratios affect the radiation properties are needed before introducing taper to an Apple-II undulator.

In this paper, simulations of the magnetic field of a tapered Apple-II undulator are performed with the computer code URCP^[17], and radiation properties of a tapered Apple-II undulator under different polarization modes are calculated and described.

2 Magnetic field simulation

An Apple-II undulator consists of four magnet arrays (Fig.1). By shifting longitudinally two of the arrays of a conventional Apple-II undulator, it provides variably polarized radiation^[10,11].

The transverse on-axis magnetic field of an Apple-II undulator can be described as^[10]:

$$B_x = B_{x0} \{ \cos[2\pi(z+z_a)/\lambda_u] - \cos[2\pi(z+z_b)/\lambda_u] - \cos[2\pi(z+z_c)/\lambda_u] + \cos[2\pi(z+z_d)/\lambda_u] \} \quad (1)$$

$$B_y = B_{y0} \{ \cos[2\pi(z+z_a)/\lambda_u] + \cos[2\pi(z+z_b)/\lambda_u] + \cos[2\pi(z+z_c)/\lambda_u] + \cos[2\pi(z+z_d)/\lambda_u] \} \quad (2)$$

where z_a , z_b , z_c , and z_d is the position shift distance of the array a, b, c and d; λ_u is the period length of Apple-II undulator; B_{x0} and B_{y0} are the on-axis peak

Supported by Shanghai Natural Science Foundation (Grant No. 08JC1422500)

* Corresponding author. E-mail address: hejianhua@sinap.ac.cn

Received date: 2008-11-17

magnetic field strength at respectively the horizontal and vertical components of a single array, and they depend on the geometric structure and material of the magnet array. Magnetic field of a single block in the magnet array can be calculated by Eq.(2). B_{x0} and B_{y0} can be calculated by superposing the magnetic field of every block in a magnet array.

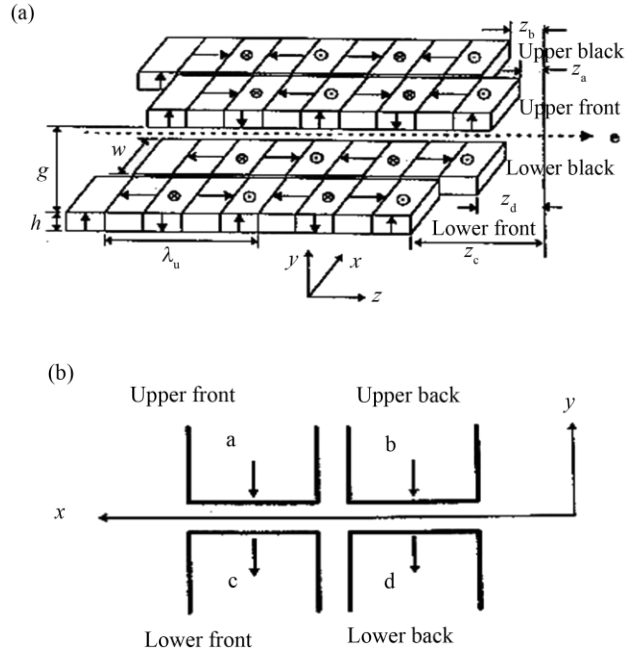


Fig.1 Magnetic array (a) and front view (b) of an Apple-II undulator^[10].

$$\begin{cases} B_x = \frac{B_r}{4\pi} \sum_{i=1}^2 \sum_{j=1}^2 \sum_{k=1}^2 (-1)^{i+j+k} \ln(R_{ijk} + y_j), \\ B_y = \frac{B_r}{4\pi} \sum_{i=1}^2 \sum_{j=1}^2 \sum_{k=1}^2 (-1)^{i+j+k} \ln(R_{ijk} + x_i), \\ B_z = -\frac{B_r}{4\pi} \sum_{i=1}^2 \sum_{j=1}^2 \sum_{k=1}^2 (-1)^{i+j+k} \arctan\left(\frac{x_i y_j}{z_k R_{ijk}}\right). \end{cases} \quad (3)$$

Here, we take EPU10 of SSRF for example. It consists of 692 magnet blocks (173 blocks for each array) in $35 \times 35 \times 25 \text{ mm}^2$ for each block. Table 1 shows the simulation results of the peak magnetic field strength in different magnetic gap^[18].

To simplify the simulations, Eq.(4) to approximately calculate B_{x0} and B_{y0} was used.

$$\begin{aligned} B_{x0} &= 0.407 \exp(-4.52g/\lambda_u - 0.0484g^2/\lambda_u^2) \\ B_{y0} &= 0.426 \exp(-3.30g/\lambda_u + 0.0214g^2/\lambda_u^2) \end{aligned} \quad (4)$$

where g is the magnetic gap in mm. As shown in Fig.2, the B_{x0} and B_{y0} calculated by Eq.(4) agree very well to the curves simulated by the URCP code, with the differences being less than 4.5% and 2.5% for B_{x0} and B_{y0} , respectively.

From Eq.(4), one finds that the B_{x0} and B_{y0} ratios vary while the gap is being tuned. Their effect on radiation properties will be evaluated in next section.

Table1 Simulated peak magnetic field strength at different magnetic gaps

Gaps(g) / mm	B_{x0} / T	B_{y0} / T
29	0.1113	0.1598
31	0.10085	0.15045
33	0.091475	0.141525
35	0.08305	0.133
37	0.07545	0.1249
39	0.068625	0.117225
41	0.062425	0.10995
43	0.05685	0.1031
45	0.0518	0.096625
47	0.0472	0.09055
49	0.04305	0.0848
51	0.0393	0.079425
53	0.035875	0.07435
55	0.032775	0.0696
57	0.02995	0.065125
59	0.027375	0.06095
61	0.025025	0.057025
63	0.0229	0.05335
65	0.02095	0.0499
67	0.0192	0.046675
69	0.017575	0.04365
71	0.0161	0.0408
73	0.014775	0.03815
75	0.013525	0.035675
77	0.012425	0.03335

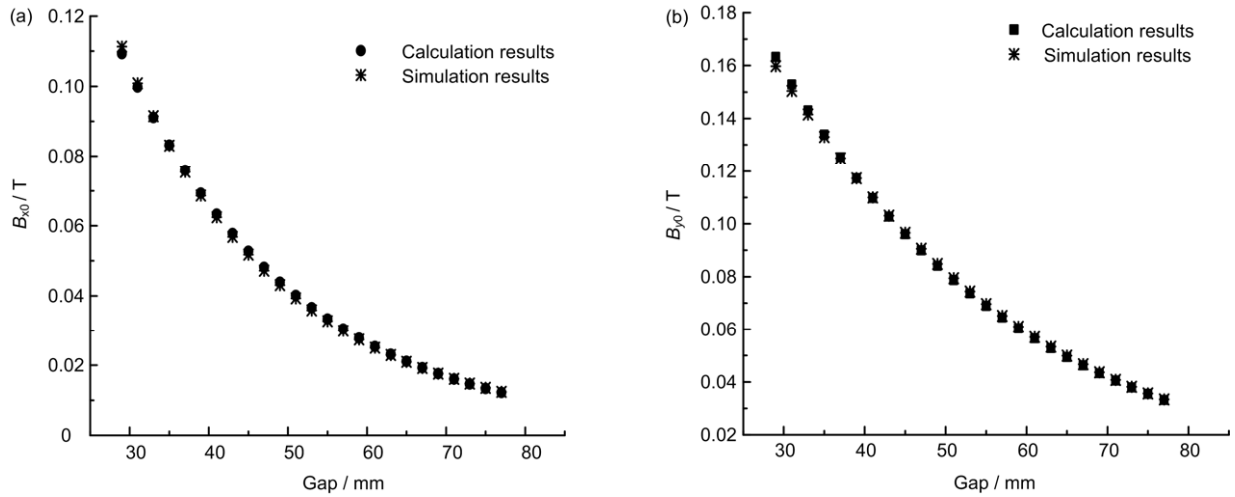


Fig.2 B_{x0} (a) and B_{y0} (b) curves calculated by Eq.(4) and simulated by the URCP code.

3 Spectral and power density distribution

The URCP^[17] code is capable of calculating many properties of the undulator radiation from arbitrary 3D magnetic field. The effect of electron beam emittance and energy spread are taken into account. Here we take the designed parameters of SSRF storage ring (Table 2)^[20] and parameter of model Apple-II undulator (Table 3) for the simulation.

Table 2 Parameters of the SSRF Storage Ring

Parameters	Values
Energy / GeV	3.5
Current/ mA	300
Natural emittance (Mode 1) / nm-rad	3.9
Natural emittance (Mode 2) / nm-rad	11.2
Coupling constant	≤ 0.01
$\beta_x/\beta_y/\eta_x$ in middle of 6.5m straight section / m	3.6/2.5/0.11
Energy spread	0.0097

Table3 Parameters of model Apple-II undulator

Period number	Period length / m	PB in the middle (B_0) / T
100	0.1	0.3

Assuming the undulator is lineally gap-tapered, we simply have:

$$g(z) = (1+\eta z/L)g_0 \quad (5)$$

where g_0 , η and z is the magnetic gap before tapering, the taper of undulator and the longitudinal position, respectively.

3.1 Vertical/horizontal linear polarization mode

When $z_a=z_b=z_c=z_d=z_0=0$, the Apple-II undulator works in the horizontal linear polarization mode, whereas it works in vertical linear polarization mode if $z_b=z_c=z_0=\lambda_u/2$, $z_a=z_d=0$. The two modes, in which the magnetic structure of a tapered Apple-II undulator is similar to a tapered planar undulator that has been well studied^[12,13] were skipped over in the simulation.

3.2 Right/left circularly polarization mode

If array b and c (Fig.1) moved to $z_a=z_d=0$, $z_b=z_c=z_0$, the Apple-II undulator works in the circularly polarization mode. The on-axis magnet field can be described as:

$$\begin{aligned} B_x &= 4B_{x0}\sin(\pi z_0/\lambda_u)\sin(2\pi z/\lambda_u + \pi z_0/\lambda_u) \\ B_y &= 4B_{y0}\cos(\pi z_0/\lambda_u)\cos(2\pi z/\lambda_u + \pi z_0/\lambda_u) \end{aligned} \quad (6)$$

where $z_0=\pm z_c=\pm(\lambda_u/\pi) \arctan (B_{y0}/B_{x0})$ and peak magnetic strength is $B_{xm} = B_{ym} = B_{x0}B_{y0}/(B_{x0}^2 + B_{y0}^2)^{1/2}$. For $\eta=0.2$, $g_0=33.3$ mm, the on-axis magnetic field can be simulated by Eqs.(3), (4) and (5). Fig.3 shows the on-axis magnetic field. The ratio of B_x and B_y amplitudes changes along the longitudinal direction.

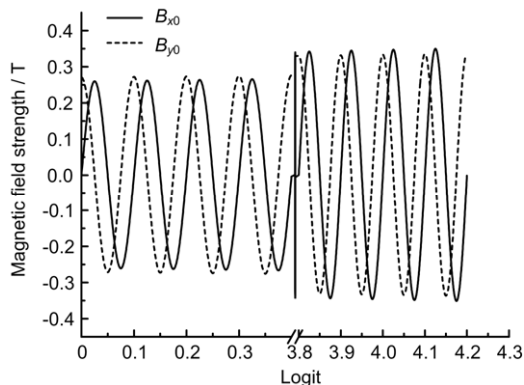


Fig.3 On-axis magnetic field of EPU10 ($\eta=0.2, g_0=33.3$ mm).

Fig.4 and Fig.5 shows the radiation properties of Apple-II undulator in tapers of different parameters given in Tables 2 and 3.

As shown in Fig.4a, energy range of the harmonics broadens and the flux density decreases with increasing tapers of the magnetic gap. Fig.4b shows the polarization spectrum of the Apple-II undulator of different tapers. The polarized degree of radiation is over 99% in the broadened energy range, with almost the same circularly polarization.

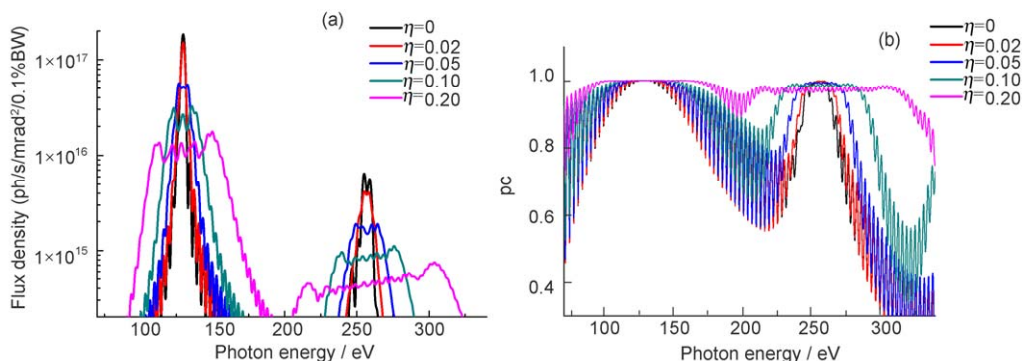


Fig.4 Spectra (a) and polarization spectra (b) of Apple-II undulator under right circularly polarization mode with different tapers.

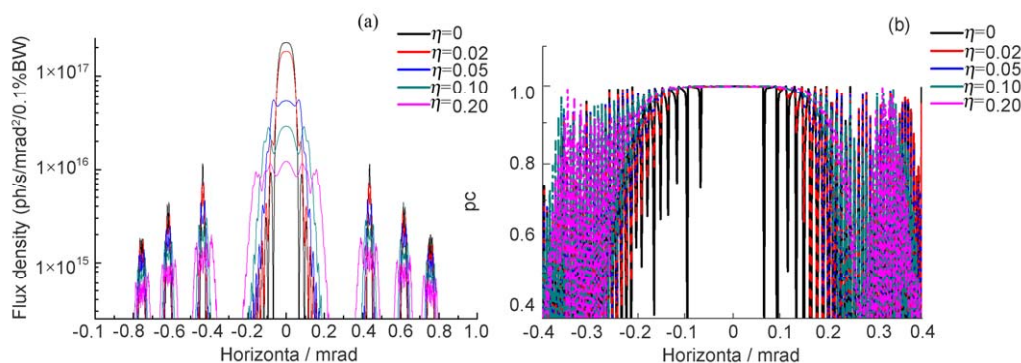


Fig.5 Spatial distribution (a) and polarization distribution (b) of Apple-II undulator of different tapers.

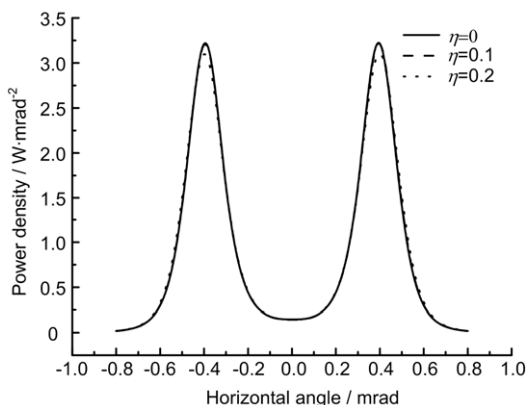


Fig.6 Power density distribution of Apple-II undulator under right circularly polarization mode of different tapers.

Fig.5a shows spatial distribution of the Apple-II undulator of different tapers. The central core is enlarged by tapering the magnetic gap. The polarized degree of radiation in the central core is more than 99% (Fig.5b).

We also calculated power density distribution of the Apple-II undulator (Fig.6). The peak power density drops slightly with the tapering magnetic gap. The effect of tapering magnetic gap on the space distribution of power density is not as remarkable as the effect on that of flux density.

3.3 The 45°/135° linear polarization mode

3.3.1 Linear polarization at 135° direction

When $-z_b=z_c=z_0$ and $z_a=z_d=0$, the on-axis magnetic field distribution can be described as

$$\begin{aligned} B_x &= 2B_{x0}[\sin(2\pi z/\lambda_u) - \sin(2\pi z/\lambda_u)\cos(2\pi z_0/\lambda_u)] \\ B_y &= 2B_{y0}[\sin(2\pi z/\lambda_u) + \sin(2\pi z/\lambda_u)\cos(2\pi z_0/\lambda_u)] \end{aligned} \quad (7)$$

If $z_0=(\lambda_u/2\pi)\arccos[(B_{x0}/B_{y0}+1)/(B_{x0}/B_{y0}-1)]$, the

polarization of radiation is linear at 135° direction, or at 45° when $z_0=(\lambda_u/2\pi)\arccos[(B_{x0}/B_{y0}-1)/(B_{x0}/B_{y0}+1)]$. In our case, $B_{x0}/B_{y0}|_{@g_0=33.3\text{mm}} = -0.646$. Therefore, the condition of $z_0=(\lambda_u/2\pi)\arccos[(-0.646-1)/(-0.646+1)]$ cannot exist and only the polarization in 135° direction at $z_0=(\lambda_u/2\pi)\arccos[(-0.646+1)/(-0.646-1)] = 28.4 \text{ mm}$ can satisfy.

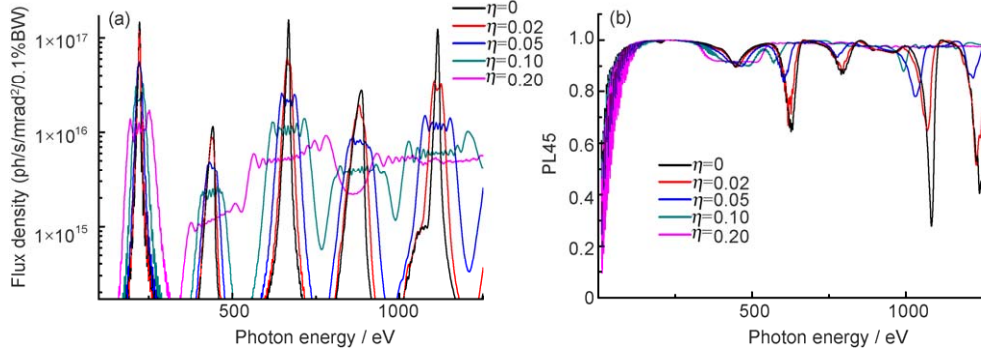


Fig.7 Spectra (a) and polarization spectra (b) of Apple-II undulator under linear polarization at 135° with different tapers.

As shown in Fig.7a, energy range of the harmonics becomes broader and the flux density decreases with increasing tapers of the magnetic gap. Fig.7b shows the polarization spectrum of Apple-II undulator of different tapers. The polarized degree of radiation is greater than 99% in the broadened energy range. So tapering an Apple-II undulator can get a broader radiation energy range with almost the same linear polarization at 135° direction.

3.3.2 Linear polarization at 45° direction

If $z_b=z_c=0$ and $-z_a=z_d=z_0$, the on-axis magnetic field distribution can be described as:

$$\begin{aligned} B_x &= -2B_{x0}[\sin(2\pi z/\lambda_u) - \sin(2\pi z/\lambda_u)\cos(2\pi z_0/\lambda_u)] \\ B_y &= 2B_{y0}[\sin(2\pi z/\lambda_u) + \sin(2\pi z/\lambda_u)\cos(2\pi z_0/\lambda_u)] \end{aligned} \quad (8)$$

If $z_0=(\lambda_u/2\pi)\arccos[(B_{x0}/B_{y0}-1)/(B_{x0}/B_{y0}+1)]$, the polarization of radiation is linear at 45° direction, or at 135° when $z_0=(\lambda_u/2\pi)\arccos[(B_{x0}/B_{y0}+1)/(B_{x0}/B_{y0}-1)]$. In our case, $B_{x0}/B_{y0}|_{@g_0=33.3\text{mm}} = -0.646$. Therefore, the condition of $z_0=(\lambda_u/2\pi)\arccos[(-0.646-1)/(-0.646+1)]$ cannot exist and only the polarization in 45° direction at $z_0=(\lambda_u/2\pi)\arccos[(-0.646+1)/(-0.646-1)] = 28.4\text{mm}$ can satisfy.

As shown in Fig.8a, the energy range of harmonic becomes broader and the flux density decreases with increasing tapers of the magnetic gap. Fig.8b shows the polarization spectrum of Apple-II undulator with different taper. The results in Figs.7 and 8 are similar.

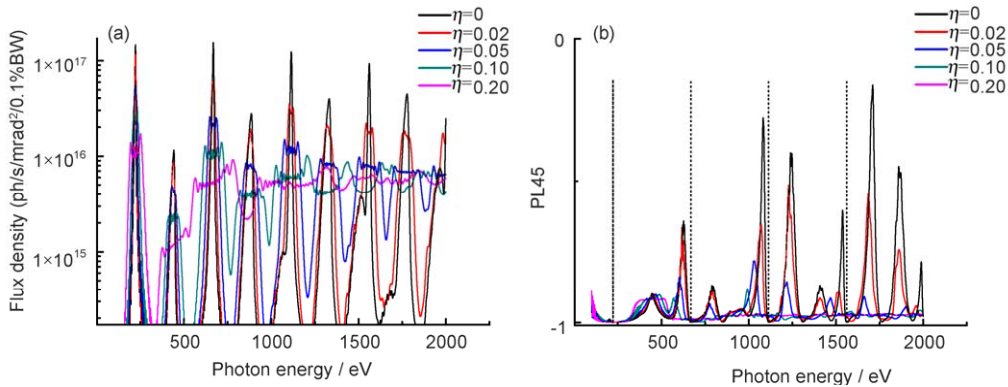


Fig.8 Spectra (a) and polarization spectra (b) of Apple-II undulator under linear polarization at 45° with different tapers.

4 Conclusion and discussion

We study the radiation properties of a tapered Apple-II undulator which have a varying ratio of B_{x0} and B_{y0} along the longitudinal direction. Previous studies focus on the tapered planar undulator or tapered helical undulator of which proportion between B_{x0} and B_{y0} stay the same along the longitudinal direction.

The calculated results demonstrate that tapering an Apple-II undulator slightly effects the polarization and power density distribution. So tapering can be introduced to Apple-II undulator in order to broaden the radiation bandwidth.

According to the simulation results, the tapered Apple-II undulator can be applied in the energy scan experiment which needs certain polarization.

References

- 1 Sasaki S. Nucl Instrum Methods Phys Res Sect A, 1994, **347**: 83–86.
- 2 Onuki H. Nucl Instrum Methods Phys Res Sect A, 1986, **246**: 94–98
- 3 Diviacco B, Walker R P. Nucl Instrum Methods Phys Res Sect A, 1990, **292**: 517–529.
- 4 Elleaume P, Chavanne J. Nucl Instrum Methods Phys Res Sect A, 1991, **304**: 719–724.
- 5 Carr R. Nucl Instrum Methods Phys Res Sect A, 1991, **306**: 391–396.
- 6 Tanaka T, Kitamura H. J Synchrotron Radiat, 1996, **3**: 47–52.
- 7 Nahon L, Corlier M, Peupardin P, *et al.* Nucl Instrum Methods Phys Res Sect A, 1997, **396**: 237–250
- 8 Dattoli G, Bucci L. Optics Communications, 2000, **177**: 323–331.
- 9 Tanaka T, Kitamura H. Nucl Instrum Methods Phys Res Sect A, 2001, **467-468**: 153–156.
- 10 Hwang C S, Yeh S. Nucl Instrum Methods Phys Res Sect A, 1999, **420**: 29–38.
- 11 Young A T, Arenholz E, Marks S, *et al.* J Synchrotron Radiat, 2002, **9**: 270–274
- 12 Lai B, Viccaro J, Dejus R J, *et al.* Rev Sci Instrum, 1993, **64**: 858–864.
- 13 Boyanov B I, Bunker G, Lee J M, *et al.* Nucl Instrum Methods Phys Res Sect A, 1994, **339**: 596–603.
- 14 Kim D E, Lee H G., Suh H S, *et al.* Nucl Instrum Methods Phys Res Sect A, 2001, **467–468**: 157–160.
- 15 Young A T, Feng J, Arenholz E, *et al.* Nucl Instrum Methods Phys Res Sect A, 2001, **467–468**: 549–552.
- 16 Bosco P, Colson W B. Phys Rev A, 1983, **28**: 319–327.
- 17 Chen M Z, He J H. Chinese phys C, 2009, **33**: 58–64.
- 18 Zhou Q G, *et al.* Report of SSRF EPU10 design, 2006.
- 19 Jackson J D, Classical Electrodynamics, Wiley, New York, 1975.
- 20 SSRF Parameters. <http://ssrf.sinap.ac.cn/1/jishu.htm>.